OCEANOGRAPHY

# Microbial rhodopsins are major contributors to the solar energy captured in the sea

**Laura Gómez-Consarnau[1,2]*, John A. Raven[3,4,5], Naomi M. Levine[2], Lynda S. Cutter[6], Deli Wang[7], Brian Seegers[8], Javier Arístegui[9], Jed A. Fuhrman[2], Josep M. Gasol[10,11], Sergio A. Sañudo-Wilhelmy[6]**

**All known phototrophic metabolisms on Earth rely on one of three categories of energy-converting pigments: chlorophyll-*a* (rarely -*d*), bacteriochlorophyll-*a* (rarely -*b*), and retinal, which is the chromophore in rhodopsins. While the significance of chlorophylls in solar energy capture has been studied for decades, the contribution of retinal-based phototrophy to this process remains largely unexplored. We report the first vertical distributions of the three energy-converting pigments measured along a contrasting nutrient gradient through the Mediterranean Sea and the Atlantic Ocean. The highest rhodopsin concentrations were observed above the deep chlorophyll-*a* maxima, and their geographical distribution tended to be inversely related to that of chlorophyll-*a*. We further show that proton-pumping proteorhodopsins potentially absorb as much light energy as chlorophyll-*a*–based phototrophy and that this energy is sufficient to sustain bacterial basal metabolism. This suggests that proteorhodopsins are a major energy-transducing mechanism to harvest solar energy in the surface ocean.**

## INTRODUCTION

Sunlight drives virtually all life on Earth's surface, with about 50% of primary productivity occurring in marine systems (*1*). However, prior to year 2000, all the known phototrophic metabolisms in the ocean were based on chlorophyll-like molecules. The discovery of marine bacterial rhodopsin-like proteins in 2000 [proteorhodopsins (PRs)] (*2*) changed the traditional concept of phototrophy radically. PRs are light-driven ion pumps that can support a variety of cellular functions, including adenosine triphosphate (ATP) synthesis (*3*), substrate uptake (*4*), and bacterial survival (*5*). Metagenomic surveys indicate that PRs are the most widespread microbial rhodopsins, with >79% of marine bacteria containing PR genes compared with only <6% containing other types of microbial rhodopsins (e.g., xanthorhodopsins and actinorhodopsins) (*6*–*9*). Recently, a new group of rhodopsins, the heliorhodopsins, was discovered in surface waters through functional metagenomics (*10*). Like other rhodopsins, heliorhodopsins capture light through a retinal chromophore and can account for as much as 20% of all microbial rhodopsins in the surface ocean (*10*). While their function in natural aquatic environments is still unknown, heliorhodopsins' slow photocycles (>1 $s^{-1}$) suggest a sensory or transport function in monoderm bacteria (*11*). Overall, metagenomic data from different environments have shown that the gene abundance of PR alone in <0.8-μm microbial fractions exceeds the combined oxygenic and anoxygenic photosystem genes by threefold (*8*, *12*). All of the available evidence strongly suggests that rhodopsin phototrophy, and that of PR in particular, is an important and widespread process in all sunlit ecosystems (*12*, *13*). However, PR quantification that relies on genes or transcripts does not necessarily reflect PR abundance. Since their discovery, only a handful of estimates of PR abundance have been reported (*14*–*18*).

To establish the ecological relevance of PRs, we directly quantified the light-sensitive pigment in microbial rhodopsins, the chromophore retinal (*19*, *20*). X-ray crystallography data show that all rhodopsins have a common structure: a typical seven-transmembrane α-helical protein motif (opsin) binding a single molecule of retinal via a covalent Schiff base (*21*–*23*). Therefore, because all the known rhodopsins have a single retinal chromophore associated with the polypeptide opsin, the total number of retinal molecules is equivalent to the total number of rhodopsins (*23*, *24*). Using this approach, we have estimated the rhodopsin concentrations in microbial communities collected along an east-west transect in the Mediterranean Sea and the Eastern Atlantic Ocean (Fig. 1A and data S1). We also compared the abundance of microbial rhodopsins to the other two major pigments, chlorophyll-*a* (Chl-*a*) for oxygenic photosynthesis and bacteriochlorophyll-*a* (Bchl-*a*) for aerobic anoxygenic phototrophy (AAP), allowing us to estimate the distribution and contribution of each of these energy-transducing mechanisms to the total solar radiation captured in the surface ocean.

## RESULTS AND DISCUSSION

To better understand the processes influencing the different phototrophic mechanisms, we collected microbial planktonic samples at different locations representing very distinct oceanographic regimes: (i) oligotrophic areas in the Eastern Mediterranean Sea (stations 2 to 12), (ii) coastal-influenced regions in the Western Mediterranean Sea (stations 13 to 24), and (iii) open ocean environments in the Eastern Atlantic Ocean (stations 25 to 29; fig. S1). Rhodopsins were found exclusively in the small microbial fraction (0.2- to 3.0-μm-size fraction), and the highest concentrations were observed above the deep chlorophyll

---

[1] Departamento de Oceanografía Biológica, Centro de Investigación Científica y de Educación Superior de Ensenada (CICESE), 22860 Ensenada, Baja California, México. [2] Department of Biological Sciences, University of Southern California, Los Angeles, CA 90089, USA. [3] Division of Plant Science, University of Dundee at the James Hutton Institute, Invergowrie, Dundee DD2 5DA, UK. [4] Climate Change Cluster, University of Technology Sydney, Ultimo, NSW 2007, Australia. [5] School of Biological Sciences, University of Western Australia, 25 Stirling Highway, Crawley, WA 6009, Australia. [6] Department of Earth Science, University of Southern California, Los Angeles, CA 90089, USA. [7] State Key Laboratory of Marine Environmental Science, Xiamen University, 422 Siming Nanlu, 361005 Xiamen, China. [8] The Scripps Research Institute, 10550 North Torrey Pines Road, La Jolla, CA 92037, USA. [9] Instituto de Oceanografía y Cambio Global (IOCAG), Universidad de Las Palmas de Gran Canaria, 35017 Las Palmas de Gran Canaria, Spain. [10] Institut de Ciències del Mar-CSIC, ES-08003 Barcelona, Catalonia, Spain. [11] Centre for Marine Ecosystems Research, School of Science, Edith Cowan University, Joondalup, WA, Australia.
*Corresponding author. Email: gomezcon@usc.edu, consarnau@cicese.mx

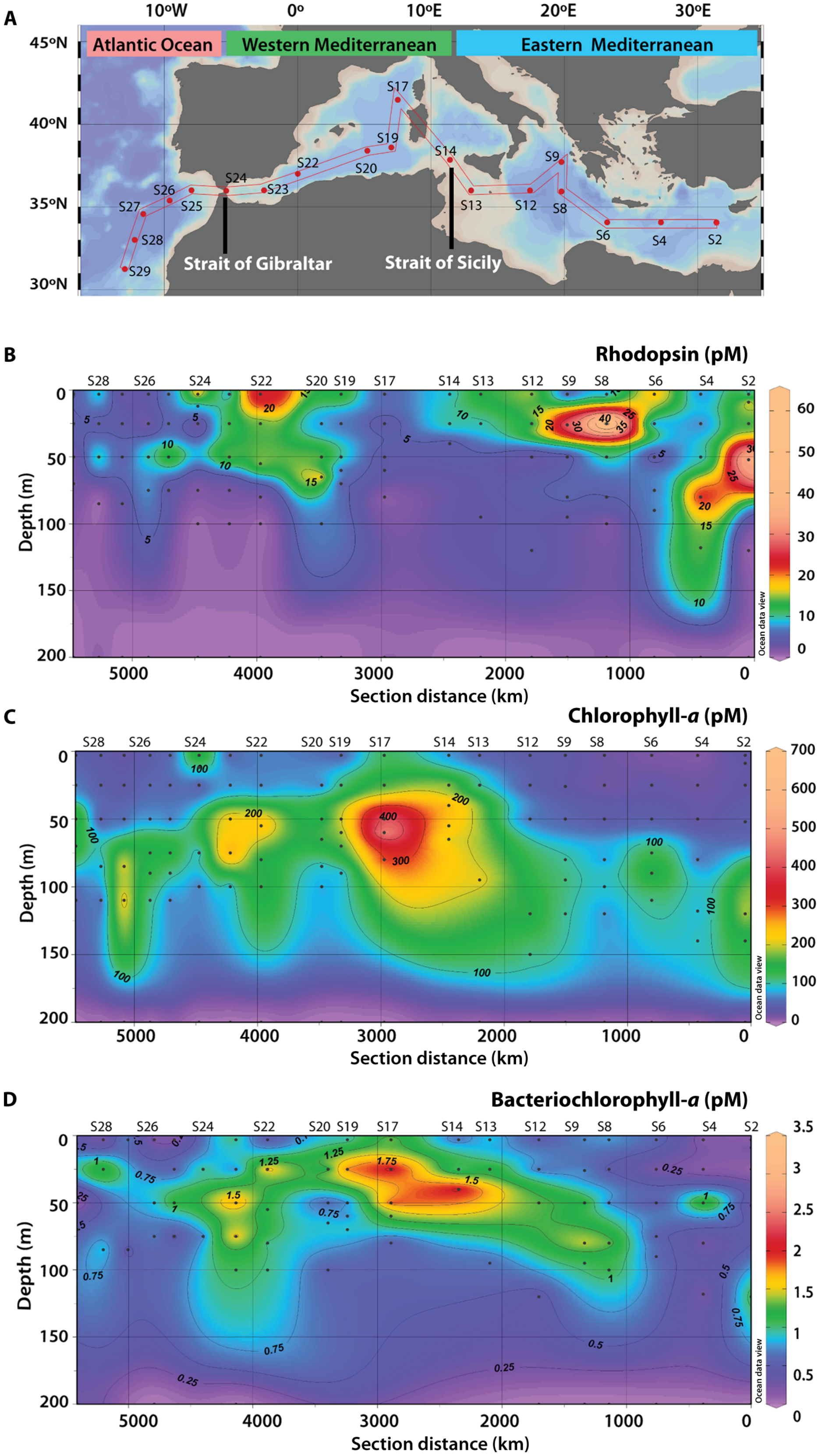

**Fig. 1. Sectional distributions of pigment concentrations measured along the Mediterranean Sea and in the Eastern Atlantic Ocean.** (**A**) Map of sampling stations. (**B**) Distribution of retinal in rhodopsins. (**C**) Chlorophyll-*a* (Chl-*a*). (**D**) Bacteriochlorophyll-*a* (Bcl-*a*). The black circles indicate the depths of sampling.

maximum in almost all stations (Figs. 1, B and C, and 2 and data S1). This may relate to the light wavelengths maximally absorbed by PRs, the most abundant microbial rhodopsins, which attenuate more rapidly in the water column than those maximally absorbed by Chl-*a* (*15*, *25*). The highest rhodopsin concentrations were observed in the low-nutrient regions of the Eastern Mediterranean Sea, with maximum values ranging from 14.4 to 61.2 pM (stations 2 to 12). This trend contrasts with the geographical distribution of Chl-*a*, which peaked in the less-oligotrophic Western Mediterranean regions (68.7 to 695.6 pM; stations 13 to 24). Therefore, the longitudinal distribution of rhodopsin photoheterotrophy showed highest values in areas where oxygenic photosynthesis was the lowest. Bchl-*a* concentrations were approximately an order of magnitude lower than those of rhodopsin throughout the entire transect (0.5 to 3.5 pM), reflecting the overall low abundance of photoheterotrophic AAP bacteria in the Mediterranean Sea (*26*, *27*). As previously observed (*27*), the highest levels of Bchl-*a* were measured in the coastal-influenced regions of the Western Mediterranean (Figs. 1D and 2). Thus, our data suggest that rhodopsin is the dominant photoheterotrophic pigment, on a molar basis, exceeding Bchl-*a* by an order of magnitude. Moreover, the observed pigment distributions support the hypothesis that rhodopsin-based phototrophy is particularly relevant in oligotrophic environments, where organic nutrients are scarce (*3*–*5*, *7*, *28*, *29*). Notably, we did not detect rhodopsin or Bchl-*a* in the 3- to 10-μm pore size fraction of any of our samples, even though rhodopsin genes and transcripts have previously been found in particle-attached bacteria and large phytoplankton (*30*–*32*). This suggests that rhodopsin-dependent metabolisms were less important for protists or for particle-attached prokaryotes than they were for the free-living picoplanktonic communities in these regions. The lack of rhodopsin in the large pore size fraction during our study also suggests that viral-like types were not present or they were in very low abundances, as the only viral rhodopsin genes identified to date belong to viruses that infect protists (*33*).

Although the rhodopsin molar concentrations measured along the oceanographic transect were about an order of magnitude lower than the levels of Chl-*a* (Fig. 1), the light-harvesting and energy transfer capabilities of each photosystem are not only a function of the absolute pigment concentrations but also depend on the number of pigment molecule clusters to form each "photosynthetic unit" (PSU; 300 molecules for Chl-*a*, 34 for Bchl-*a*, and 1 for rhodopsin) (*22*, *34*, *35*). Rhodopsin displayed the highest concentration of PSUs ($1 \times 10^{11}$ to $4 \times 10^{13}$ PSU $L^{-1}$), exceeding those of Chl-*a* by an order of magnitude ($1 \times 10^{10}$ to $1 \times 10^{12}$ PSU $L^{-1}$; data S1). The concentration of PSUs for Bchl-*a* was several orders of magnitude lower than those of rhodopsin and Chl-*a* ($2 \times 10^{9}$ to $7 \times 10^{10}$ PSU $L^{-1}$; data S1). We further estimated the amounts of depth-integrated energy potentially captured by rhodopsin phototrophy, Chl-*a*–based photosynthesis, and Bchl-*a*–based AAP in the water column (in kJ $m^{-2}$ $day^{-1}$; Fig. 3 and data S1). To account only for light-driven proton-pumping PRs, which are the rhodopsin types involved in cellular energetics, only 80% of the retinal signal was used for these calculations (see Supplementary Materials and Methods). This correction assumes that 20% of the total retinal measured in our samples is from the recently discovered and widespread heliorhodopsins that also contain the retinal chromophore (*10*). Consistent with the spatial trends observed in the concentration of PSUs across the transect, we found that PR had the potential to capture the highest amount of radiant energy in all stations except one, ranging from 11 to 107 kJ $m^{-2}$ $day^{-1}$. These estimates are about an order of magnitude higher than the depth-integrated solar energy captured by oxygenic photosynthesis by autotrophic phytoplankton in the Eastern Mediterranean (Chl-*a*–based energy range, 2 to 19 kJ $m^{-2}$ $day^{-1}$). In contrast, the extent of solar radiation absorbed by AAP bacteria (0.04 to 0.78 kJ $m^{-2}$ $day^{-1}$) was orders of magnitude lower than that absorbed through the other two photosystems. These patterns were consistent regardless of whether the pigment-specific absorbance wavelengths or the total

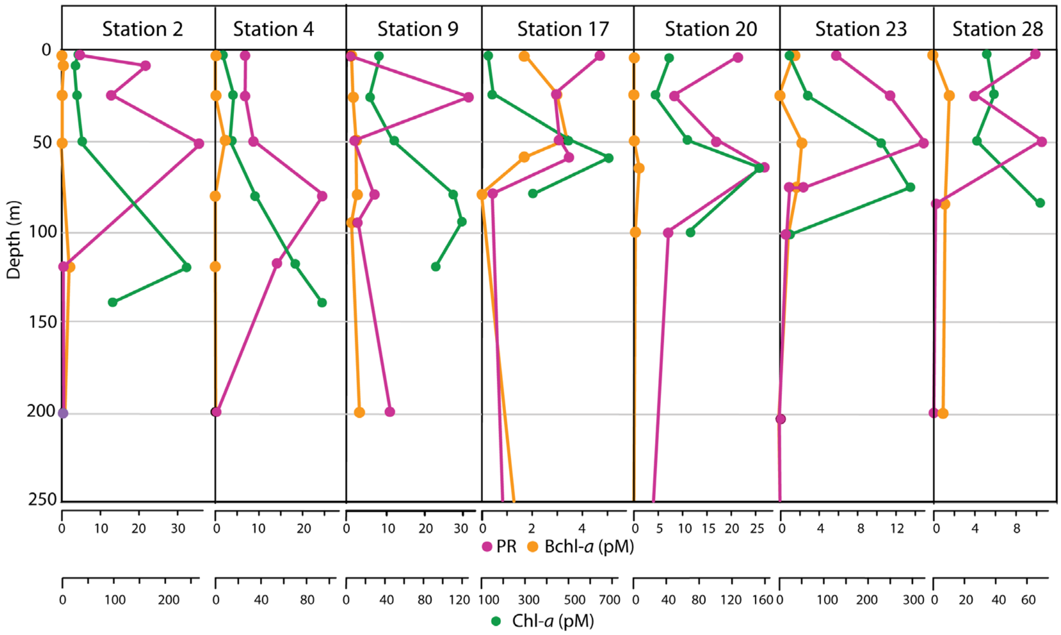

**Fig. 2. Depth profiles of pigment concentrations (rhodopsin retinal, Bchl-*a*, and Chl-*a*) measured at the different basins of the Mediterranean Sea and Eastern Atlantic Ocean.** Stations 2, 4, and 9 are representative of oligotrophic regions of the Eastern Mediterranean; stations 17, 20, and 23 were sampled in the coastal-influenced Western Mediterranean; and station 28 was sampled in the Eastern Atlantic Ocean.

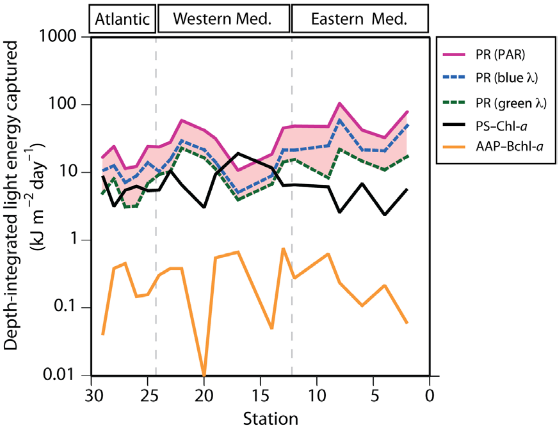

**Fig. 3. Geographical distribution of the depth-integrated light energy captured by PR, Chl-*a* photosystem (PS–Chl-*a*), and AAP–Bchl-*a* at the different sampling regions of the Mediterranean Sea and Eastern Atlantic Ocean within the photic zone (0 to 200 m).** A photocycle of 10 ms was used for the PR calculations, as DNA sequence, spectral tuning, and kinetics data (*6*, *44*) show that most PRs from surface temperate waters have fast photocycles typical of $H^+$ pumps. To account for any retinal signal originating from heliorhodopsin, which could represent ~20% of all rhodopsins in the photic zone (*10*), 80% of the quantified retinal signal was used in these calculations. Solid lines denote estimates using all PAR (400 to 700 nm). Those represent the maximum energy estimates, which assume that also accessory pigments can access all wavelengths (PAR; 400 to 700 nm). Conservative energy calculations using specific wavelengths for blue-absorbing (490 nm) and green-absorbing (530 nm) PR are shown in dashed lines.

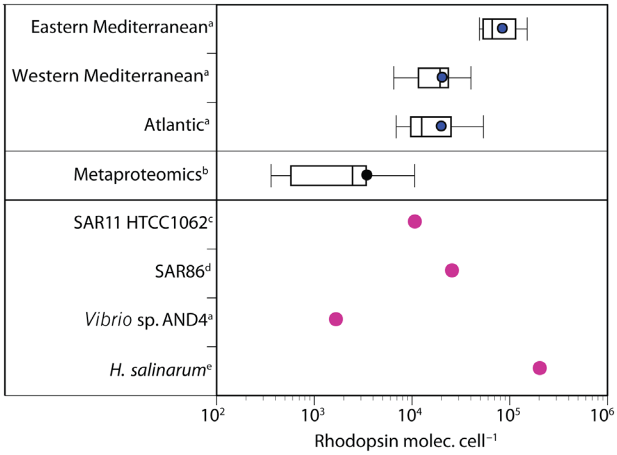

**Fig. 4. Rhodopsin cellular quotas (molecules cell$^{-1}$) measured in the picoplankton collected in the different basins of the Mediterranean Sea and in the Eastern Atlantic Ocean compared with prior studies.** $^a$Samples measured in this study: Eastern Mediterranean (stations 2 to 12), Western Mediterranean (stations 13 to 24), and Atlantic Ocean (stations 25 to 29) and *Vibrio* sp. AND4; $^b$metaproteomics estimates from (*16*); laser flash photolysis measurements: $^c$SAR11 bacterium *Candidatus* Pelagibacter ubique HTCC1062 (*17*), $^d$SAR86 bacteria (*15*), and $^e$*Halobacterium salinarum* (*38*). The line within the boxplot is the median, the dot is the mean, and the boundary of the boxes indicates the 25th and 75th percentiles. Error bars to the left and to the right of the box indicate the 10th and 90th percentiles.

photosynthetically available radiant (PAR) energy was used in our calculations (data S1). By considering the incident photon flux density in the visible spectrum (PAR, 400 to 700 nm), these calculations account for photons potentially harvested by accessory pigments in antenna complexes during photosynthesis using Chl-*a* in the reaction centers, as well as the predominant blue (Soret) absorption bands of antenna bacteriochlorophylls, and carotenoids, with Bchl-*a* in the reaction center (*36*, *37*).

The spatial gradient of cellular rhodopsin concentrations (molecules cell$^{-1}$) observed in our samples further confirms that retinal-based photoheterotrophy is particularly favored in the nutrient-limited areas of the Mediterranean (Fig. 4). For example, the cellular rhodopsin content measured in the oligotrophic picoplankton from the Eastern Mediterranean ranged from 45,000 to 145,000 molecules cell$^{-1}$, exceeding by almost an order of magnitude earlier estimates (*16*). Similar rhodopsin quotas have only been observed previously in Haloarchaea species from hypersaline environments (*38*). In contrast, cellular rhodopsin content in the Eastern Atlantic Ocean (6000 to 50,000 molecules cell$^{-1}$) and the Western Mediterranean Sea (6000 to 39,000 molecules cell$^{-1}$) were on the same range as previous measurements in both environmental and pure culture samples (Fig. 4). These results imply that the spatial distribution in the rhodopsin cellular content is related to inorganic nutrient concentrations (fig. S1), suggesting that the characteristics of different nutrient regimes might have a profound impact on the type of metabolism (heterotrophy versus phototrophy) used by photoheterotrophic bacteria.

To evaluate the possible physiological advantages provided by photoheterotrophy to rhodopsin-containing bacteria, we estimated the potential highest energy yields on a per-cell basis provided by PR (in kJ cell$^{-1}$ day$^{-1}$; Fig. 5). These energy estimates were also corrected by the retinal potentially present in heliorhodopsins (see Supplementary Materials and Methods). The highest cellular energy yield from PR ranged from $5.62 \times 10^{-14}$ to $1.13 \times 10^{-12}$ kJ cell$^{-1}$ day$^{-1}$ along the Mediterranean Sea–Atlantic Ocean transect. Those PR energy per-cell yields were substantially lower than the energy provided by Chl-*a* ($3.90 \times 10^{-11}$ to $9.16 \times 10^{-13}$ kJ cell$^{-1}$ day$^{-1}$). However, with far more PR-containing cells than chlorophyll-containing ones, the cumulative or depth-integrated energy capture from PR was larger, as shown above (Fig. 3). Our calculations also showed that the cellular energy yield captured by PR was within or below the minimum energy threshold required for survival in heterotrophic bacteria ($2 \times 10^{-13}$ to $4 \times 10^{-13}$ kJ cell$^{-1}$ day$^{-1}$) (*16*). However, at some locations in the Eastern Mediterranean, the energy acquired by PR was above that threshold by an order of magnitude (Fig. 5). Together, these results suggest that PR alone could provide, at least, enough energy to each individual bacterium, on average, to sustain its basal metabolism. From the perspective of photoheterotrophy, our per-cell energy calculations are consistent with the fact that known AAP- and PR-containing bacteria are still heterotrophs and require organic matter for biomass synthesis or growth. These data also support the hypothesis that the most extremely oligotrophic marine environments (e.g., Eastern Mediterranean) have such low primary production from photosynthesis that complementary light-dependent metabolisms can supply as much or possibly more energy to heterotrophic prokaryotes than they can obtain from organic matter through classic food web–based energy transfers.

Overall, the observed geographical trends observed in our study support the notion that rhodopsin photoheterotrophy, and PR in particular, is a particularly important mechanism for bacterioplankton survival in areas where other resources are scarce (*3*–*5*, *28*, *29*). So, while PR-containing taxa are found in low- and high-nutrient-concentration waters worldwide (*7*), this mechanism is exceptionally valuable in sunlit oligotrophic locations, possibly including the South Pacific Gyre, an area much larger than the Eastern Mediterranean. Last, although we were not able to determine how much of the harvested solar energy was

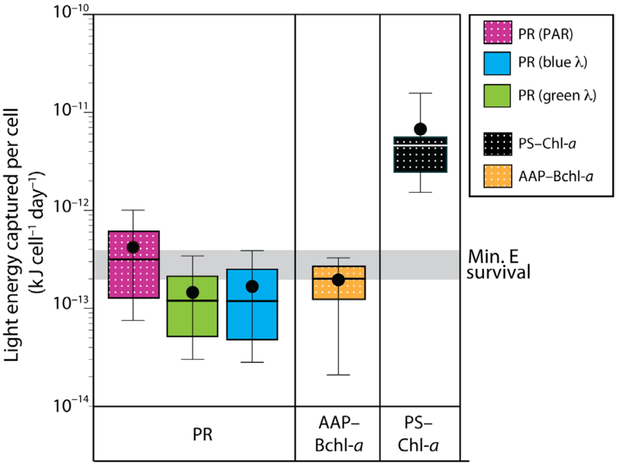

**Fig. 5. Light energy captured per cell by PR, Bchl-*a* (AAP–Bchl-*a*), and Chl-*a* (PS–Chl-*a*) in the Mediterranean Sea and Eastern Atlantic Ocean.** These calculations assumed hyperbolic response to light, that 75% of the total heterotrophic bacteria contain PR genes and 2.5% contain Bchl-*a* (see Supplementary Materials and Methods and table S5). To account for any retinal signal originating from heliorhodopsin, which could represent ~20% of all rhodopsins in the photic zone (*10*), 80% of the quantified retinal signal was used in these calculations. Chl-*a*–containing cells were estimated as the addition of the *Prochlorococcus*, *Synechococcus*, and picoeukaryote counts measured with flow cytometry. As reference, the gray horizontal band denotes the estimated energy range necessary to maintain basal metabolism or survival in heterotrophic bacteria (*16*). Dotted boxes denote estimates using all PAR (400 to 700 nm). Conservative calculations using only specific wavelengths for blue-absorbing (490 nm) and green-absorbing (530 nm) PR are shown as blue and green boxes.

transformed into actual biological functions such as light-enhanced substrate uptake (*4*) or ATP synthesis (*3*), our results suggest that PR photoheterotrophy captures and potentially channels substantial amounts of radiant energy to the biosphere. Future challenges will include understanding to what extent and in which manner this prevailing type of phototrophy affects the processing of organic matter and, therefore, its role in the marine carbon cycle. The estimated large contribution of PRs to the energy budget in less-productive regions suggests that retinal-based phototrophy is likely to increase as oligotrophic areas continue to expand in the world ocean in response to climate change forcing (*39*).

## MATERIALS AND METHODS

Seawater samples were collected along a Mediterranean Sea–Atlantic Ocean transect (Fig. 1) on board the Spanish ship *RV Sarmiento de Gamboa* from 30 April to 28 May 2014. Sampling dates and station coordinates are given in data S1. Samples were collected at various depths within the photic zone using a CTD (conductivity-temperature-depth profiler) rosette equipped with 12-liter Niskin bottles. For the retinal and Bchl-*a* analyses, 8 liters of seawater were filtered per depth using a peristaltic pump connected to a sequential filtration system. To avoid the presence of large planktonic organisms in the samples, water was prescreened using a nylon 10-μm mesh attached to the inflow of the filtration system. The 3- to 10-μm and the 3- to 0.2-μm microbial-size fractions were collected using 47-mm diameter 3-μm pore size polycarbonate filters (Millipore Corp., Billerica, MA) and 0.2-μm pore size Sterivex-GV filter units (Millipore), respectively. Filters were stored at −80°C until extraction. The retinal extraction and analysis protocol was modified from the literature (*19*, *20*) and optimized for marine samples using cultures of the PR-containing bacterium *Vibrio* sp. AND4 and the knockout mutant strain AND4-Δ*prd* (*5*) (see Supplementary Materials and Methods). Briefly, the filters were sonicated in 3 ml of liquid chromatography–mass spectrometry (LC-MS)–grade methanol on ice and in the dark for 30 s. Butylated hydroxytoluene (1%; 250 μl) was subsequently added, and the samples were left to extract for 24 hours at −20°C. After the extraction, a 0.5-ml aliquot was used for Bchl-*a* analysis by high-performance liquid chromatography (*40*). Hydroxylamine (1 M; 100 μl) was added to the remaining sample extraction and was incubated under light for 2 hours. PR concentration was determined as total retinal oxime, which is the transformation product of reacting retinal (either *cis* or all-*trans* isoform) with hydroxylamine, using LC-MS (triple-quadrupole LC-MS/MS). The technique is fully described in the Supplementary Materials and Methods. For Chl-*a* measurements, 500 ml of seawater was filtered through 25-mm GF/F filters (Whatman) using low vacuum. The filters were frozen at −20°C before pigments were extracted on board in 90% acetone for 24 hours in the dark at 4°C. Chl-*a* concentrations were estimated by fluorometry in a Turner Designs fluorometer calibrated with pure Chl-*a* (Sigma Chemical) (*41*). Dissolved inorganic nutrients (nitrate and phosphate) were collected from the Niskin bottles in 20-ml acid-washed polyethylene flasks and determined on board using standard segmented flow analysis methods with colorimetric detection measured on board (*42*). Autotrophic picoplankton (*Prochlorococcus*, *Synechococcus*, and picoeukaryotes) and heterotrophic prokaryotes were enumerated by flow cytometry (Becton Dickinson FACSCalibur) (*43*). The bioenergetic calculations used to determine the radiant energy captured by PR assume that 80% of the quantified retinal belonged to proton-pumping PRs (*10*), and more details can be found in the Supplementary Materials and Methods. Any other potential retinal sources present in seawater but unknown to date cannot be accounted for at this stage of environmental retinal research and might need to be evaluated in the future.

## SUPPLEMENTARY MATERIALS

Supplementary material for this article is available at http://advances.sciencemag.org/cgi/content/full/5/8/eaaw8855/DC1

Supplementary Materials and Methods

Fig. S1. Inorganic nutrient concentrations measured along the Mediterranean Sea and East Atlantic Ocean.

Fig. S2. Retinal oxime reextraction test.

Fig. S3. Concentrations of retinal oxime in *Vibrio* sp. AND4 extracted using hydroxylamine under different light conditions.

Fig. S4. Retinal extraction time optimization in *Vibrio* sp. AND4.

Fig. S5. Number of retinal molecules (as retinal oxime) measured in the *Vibrio* sp. AND4 wild-type (wt) and in the knockout mutant strain (Δ*prd*).

Fig. S6. Concentration of rhodopsin-bound retinal (as retinal oxime) measured in surface waters collected in January 2015 at station SPOT.

Fig. S7. Contribution of the potential energy captured by PRs at different depths.

Table S1. Summary of treatments used to optimize the extraction and detection of retinal, retinal oxime, and Bchl-*a*.

Table S2. Transformation of retinal into retinal oxime using all-*trans* retinal standards.

Table S3. Light wavelength characteristics.

Table S4. Parameters used to calculate the light energy captured shown in Figs. 3 and 5.

Table S5. Parameters used to calculate the cellular daily energy yield per photosystem shown in Fig. 5 and data S1.

Data S1. Detailed sampling measurements and calculations obtained in the Mediterranean Sea and East Atlantic Ocean from 30 April to 28 May 2014.

References (*45*–*55*)

## REFERENCES AND NOTES

1. P. G. Falkowski, The role of phytoplankton photosynthesis in global biogeochemical cycles. *Photosynth. Res.* **39**, 235–258 (1994).
2. O. Béjà, L. Aravind, E. V. Koonin, M. T. Suzuki, A. Hadd, L. P. Nguyen, S. B. Jovanovich, C. M. Gates, R. A. Feldman, J. L. Spudich, E. N. Spudich, E. F. DeLong, Bacterial rhodopsin: Evidence for a new type of phototrophy in the sea. *Science* **289**, 1902–1906 (2000).

3. L. Steindler, M. S. Schwalbach, D. P. Smith, F. Chan, S. J. Giovannoni, Energy Starved *Candidatus* Pelagibacter Ubique Substitutes Light-Mediated ATP Production for Endogenous Carbon Respiration. *PLOS ONE* **6**, e19725 (2011).
4. L. Gómez-Consarnau, J. M. González, T. Riedel, S. Jaenicke, I. Wagner-Döbler, S. A. Sañudo-Wilhelmy, J. A. Fuhrman, Proteorhodopsin light-enhanced growth linked to vitamin-$B_1$ acquisition in marine Flavobacteria. *ISME J.* **10**, 1102–1112 (2016).
5. L. Gómez-Consarnau, N. Akram, K. Lindell, A. Pedersen, R. Neutze, D. L. Milton, J. M. González, J. Pinhassi, Proteorhodopsin phototrophy promotes survival of marine bacteria during starvation. *PLOS Biol.* **8**, e1000358 (2010).
6. G. Sabehi, A. Loy, K.-H. Jung, R. Partha, J. L. Spudich, T. Isaacson, J. Hirschberg, M. Wagner, O. Béjà, New insights into metabolic properties of marine bacteria encoding proteorhodopsins. *PLOS Biol.* **3**, e273 (2005).
7. D. B. Rusch, A. L. Halpern, G. Sutton, K. B. Heidelberg, S. Williamson, S. Yooseph, D. Wu, J. A. Eisen, J. M. Hoffman, K. Remington, K. Beeson, B. Tran, H. Smith, H. Baden-Tillson, C. Stewart, J. Thorpe, J. Freeman, C. Andrews-Pfannkoch, J. E. Venter, K. Li, S. Kravitz, J. F. Heidelberg, T. Utterback, Y.-H. Rogers, L. I. Falcón, V. Souza, G. Bonilla-Rosso, L. E. Eguiarte, D. M. Karl, S. Sathyendranath, T. Platt, E. Bermingham, V. Gallardo, G. Tamayo-Castillo, M. R. Ferrari, R. L. Strausberg, K. Nealson, R. Friedman, M. Frazier, J. C. Venter, The Sorcerer II Global Ocean Sampling Expedition: Northwest Atlantic through Eastern Tropical Pacific. *PLOS Biol.* **5**, e77 (2007).
8. V. Dubinsky, M. Haber, I. Burgsdorf, K. Saurav, Y. Lehahn, A. Malik, D. Sher, D. Aharonovich, L. Steindler, Metagenomic analysis reveals unusually high incidence of proteorhodopsin genes in the ultraoligotrophic Eastern Mediterranean Sea. *Environ. Microbiol.* **19**, 1077–1090 (2017).
9. E. T. Sieradzki, J. A. Fuhrman, S. Rivero-Calle, L. Gómez-Consarnau, Proteorhodopsins dominate the expression of phototrophic mechanisms in seasonal and dynamic marine picoplankton communities. *PeerJ* **6**, e5798 (2018).
10. A. Pushkarev, K. Inoue, S. Larom, J. Flores-Uribe, M. Singh, M. Konno, S. Tomida, S. Ito, R. Nakamura, S. P. Tsunoda, A. Philosof, I. Sharon, N. Yutin, E. V. Koonin, H. Kandori, O. Béjà, A distinct abundant group of microbial rhodopsins discovered using functional metagenomics. *Nature* **558**, 595–599 (2018).
11. J. Flores-Uribe, G. Hevroni, R. Ghai, A. Pushkarev, K. Inoue, H. Kandori, O. Béjà, Heliorhodopsins are absent in diderm (Gram-negative) bacteria: Some thoughts and possible implications for activity. *Environ. Microbiol. Rep.* **11**, 419–424 (2019).
12. O. M. Finkel, O. Béjà, S. Belkin, Global abundance of microbial rhodopsins. *ISME J.* **7**, 448–451 (2013).
13. N. Atamna-Ismaeel, O. M. Finkel, F. Glaser, I. Sharon, R. Schneider, A. F. Post, J. L. Spudich, C. von Mering, J. A. Vorholt, D. Iluz, O. Béjà, S. Belkin, Microbial rhodopsins on leaf surfaces of terrestrial plants. *Environ. Microbiol.* **14**, 140–146 (2012).
14. J. A. Raven, Functional evolution of photochemical energy transformations in oxygen-producing organisms. *Funct. Plant Biol.* **36**, 505–515 (2009).
15. O. Béjà, E. N. Spudich, J. L. Spudich, M. Leclerc, E. F. DeLong, Proteorhodopsin phototrophy in the ocean. *Nature* **411**, 786–789 (2001).
16. D. L. Kirchman, T. E. Hanson, Bioenergetics of photoheterotrophic bacteria in the oceans. *Environ. Microbiol. Rep.* **5**, 188–199 (2013).
17. S. J. Giovannoni, L. Bibbs, J.-C. Cho, M. D. Stapels, R. Desiderio, K. L. Vergin, M. S. Rappé, S. Laney, L. J. Wilhelm, H. J. Tripp, E. J. Mathur, D. F. Barofsky, Proteorhodopsin in the ubiquitous marine bacterium SAR11. *Nature* **438**, 82–85 (2005).
18. J. L. Keffer, C. R. Sabanayagam, M. E. Lee, E. F. DeLong, M. W. Hahn, J. A. Maresca, Using total internal reflection fluorescence microscopy to visualize rhodopsin-containing cells. *Appl. Environ. Microbiol.* **81**, 3442–3450 (2015).
19. D. Oesterhelt, W. Stoeckenius, Isolation of the cell membrane of Halobacterium halobium and its fractionation into red and purple membrane. *Methods Enzymol.* **31**, 667–678 (1974).
20. W. S. M. El-Sayed, S. Takaichi, H. Saida, M. Kamekura, M. Abu-Shady, H. Seki, T. Kuwabara, Effects of light and low oxygen tension on pigment biosynthesis in *Halobacterium salinarum*, revealed by a novel method to quantify both retinal and carotenoids. *Plant Cell Physiol.* **43**, 379–383 (2002).
21. H. Luecke, B. Schobert, H.-T. Richter, J.-P. Cartailler, J. K. Lanyi, Structural changes in bacteriorhodopsin during ion transport at 2 angstrom resolution. *Science* **286**, 255–260 (1999).
22. O. P. Ernst, D. T. Lodowski, M. Elstner, P. Hegemann, L. S. Brown, H. Kandori, Microbial and animal rhodopsins: Structures, functions, and molecular mechanisms. *Chem. Rev.* **114**, 126–163 (2014).
23. J. Pinhassi, E. F. DeLong, O. Béjà, J. M. Gonzalez, C. Pedrós-Alió, Marine bacterial and archaeal ion-pumping rhodopsins: Genetic diversity, physiology, and ecology. *Microbiol. Mol. Biol. Rev.* **80**, 929–954 (2016).
24. D. Oesterhelt, W. Stoeckenius, Rhodopsin-like protein from the purple membrane of *Halobacterium halobium*. *Nat. New Biol.* **233**, 149–152 (1971).
25. P. G. Falkowski, J. A. Raven, *Aquatic Photosynthesis* (Blackwell Science, Malden, MA, 1997).
26. E. Hojerová, M. Mašín, C. Brunet, I. Ferrera, J. M. Gasol, M. Koblížek, Distribution and growth of aerobic anoxygenic phototrophs in the Mediterranean Sea. *Environ. Microbiol.* **13**, 2717–2725 (2011).
27. D. Lamy, C. Jeanthon, M. T. Cottrell, D. L. Kirchman, F. van Wambeke, J. Ras, O. Dahan, M. Pujo-Pay, L. Oriol, L. Bariat, P. Catala, V. Cornet-Barthaux, P. Lebaron, Ecology of aerobic anoxygenic phototrophic bacteria along an oligotrophic gradient in the Mediterranean Sea. *Biogeosciences* **8**, 973–985 (2011).
28. L. Gómez-Consarnau, J. M. González, M. Coll-Lladó, P. Gourdon, T. Pascher, R. Neutze, C. Pedrós-Alió, J. Pinhassi, Light stimulates growth of proteorhodopsin-containing marine Flavobacteria. *Nature* **445**, 210–213 (2007).
29. R. M. Morris, B. L. Nunn, C. Frazar, D. R. Goodlett, Y. S. Ting, G. Rocap, Comparative metaproteomics reveals ocean-scale shifts in microbial nutrient utilization and energy transduction. *ISME J.* **4**, 673–685 (2010).
30. C. H. Slamovits, N. Okamoto, L. Burri, E. R. James, P. J. Keeling, A bacterial proteorhodopsin proton pump in marine eukaryotes. *Nat. Commun.* **2**, 183 (2011).
31. A. Marchetti, D. Catlett, B. M. Hopkinson, K. Ellis, N. Cassar, Marine diatom proteorhodopsins and their potential role in coping with low iron availability. *ISME J.* **9**, 2745–2748 (2015).
32. J. A. Maresca, K. J. Miller, J. L. Keffer, C. R. Sabanayagam, B. J. Campbell, Distribution and diversity of rhodopsin-producing microbes in the Chesapeake Bay. *Appl. Environ. Microbiol.* **84**, e00137–18 (2018).
33. N. Yutin, E. V. Koonin, Proteorhodopsin genes in giant viruses. *Biol. Direct* **7**, 34 (2012).
34. P. Horton, A. V. Ruban, R. G. Walters, Regulation of light harvesting in green plants. *Annu. Rev. Plant. Physiol. Plant. Mol. Biol.* **47**, 655–684 (1996).
35. V. V. Yurkov, J. T. Beatty, Aerobic anoxygenic phototrophic bacteria. *Microbiol. Mol. Biol. Rev.* **62**, 695–724 (1998).
36. J. K. Lanyi, S. P. Balashov, Xanthorhodopsin: A bacteriorhodopsin-like proton pump with a carotenoid antenna. *Biochim. Biophys. Acta* **1777**, 684–688 (2008).
37. A. W. D. Larkum, R. J. Ritchie, J. A. Raven, Living off the Sun: Chlorophylls, bacteriochlorophylls and rhodopsins. *Photosynthetica* **56**, 11–43 (2018).
38. R. A. Bogomolni, J. L. Spudich, Identification of a third rhodopsin-like pigment in phototactic *Halobacterium halobium*. *Proc. Natl. Acad. Sci. U.S.A.* **79**, 6250–6254 (1982).
39. J. J. Polovina, E. A. Howell, M. Abecassis, Ocean's least productive waters are expanding. *Geophys. Res. Lett.* **35**, L03618 (2008).
40. R. Goericke, Bacteriochlorophyll a in the ocean: Is anoxygenic bacterial photosynthesis important? *Limnol. Oceanogr.* **47**, 290–295 (2002).
41. O. Holm-Hansen, C. J. Lorenzen, R. W. Holmes, J. D. H. Strickland, Fluorometric determination of chlorophyll. *ICES J. Mar. Sci.* **30**, 3–15 (1965).
42. K. Kremling, M. O. Andreae, L. Brügmann, C. M. G. van den Berg, A. Prange, M. Schirmacher, E. Koroleff, J. Kuss, Determination of trace elements, in *Methods of Seawater Analysis*, K. Grasshoff, M. Ehrhardt, K. Kremling, Eds. (Wiley-VCH Verlag GmbH, 2007), pp. 253–364.
43. J. M. Gasol, P. A. Del Giorgio, Using flow cytometry for counting natural planktonic bacteria and understanding the structure of planktonic bacterial communities. *Sci. Mar.* **64**, 197–224 (2000).
44. J. Y. Jung, A. R. Choi, Y. K. Lee, H. K. Lee, K.-H. Jung, Spectroscopic and photochemical analysis of proteorhodopsin variants from the surface of the Arctic Ocean. *FEBS Lett.* **582**, 1679–1684 (2008).
45. J. E. Hobbie, R. J. Daley, S. Jasper, Use of nuclepore filters for counting bacteria by fluorescence microscopy. *Appl. Environ. Microbiol.* **33**, 1225–1228 (1977).
46. M. A. Kane, J. L. Napoli, Quantification of endogenous retinoids. *Methods Mol. Biol.* **652**, 1–54 (2010).
47. X. Wu, J. Jiang, Y. Wan, J. P. Giesy, J. Hu, Cyanobacteria blooms produce teratogenic retinoic acids. *Proc. Natl. Acad. Sci. U.S.A.* **109**, 9477–9482 (2012).
48. R. B. Stull, *An Introduction to Boundary Layer Meteorology* (Kluwer Academic Publishers, Boston, MA, 1988), vol. 13, pp. 404.
49. K. E. Bailey, D. A. Toole, B. Blomquist, R. G. Najjar, B. Huebert, D. J. Kieber, R. P. Kiene, P. Matrai, G. R. Westby, D. A. del Valle, Dimethylsulfide production in Sargasso Sea eddies. *Deep Sea Res. Part 2 Top. Stud. Oceanogr.* **55**, 1491–1504 (2008).
50. J. M. Walter, D. Greenfield, C. Bustamante, J. Liphardt, Light-powering *Escherichia coli* with proteorhodopsin. *Proc. Natl. Acad. Sci. U.S.A.* **104**, 2408–2412 (2007).
51. M. Koblížek, Ecology of aerobic anoxygenic phototrophs in aquatic environments. *FEMS Microbiol. Rev.* **39**, 854–870 (2015).
52. J. A. Raven, *Energetics and Transport in Aquatic Plants* (A. R. Liss, NY, 1984).
53. J. A. Raven, J. Beardall, M. Giordano, Energy costs of carbon dioxide concentrating mechanisms in aquatic organisms. *Photosynth. Res.* **121**, 111–124 (2014).
54. R. R. Bidigare, M. E. Ondrusek, J. H. Morrow, D. A. Kiefer, In-vivo absorption properties of algal pigments, in *Orlando'90*, R. W. Spinrad, Ed. (1990), pp. 290–302.
55. Z. S. Kolber, F. G. Plumley, A. S. Lang, J. T. Beatty, R. E. Blankenship, C. VanDover, C. Vetriani, M. Koblizek, C. Rathgeber, P. G. Falkowski, Contribution of aerobic photoheterotrophic bacteria to the carbon cycle in the ocean. *Science* **292**, 2492–2495 (2001).

**Acknowledgments:** We thank X. A. Alvarez-Salgado and V. Vieitez for the inorganic nutrient data, the crew on board the vessel Sarmiento de Gamboa for sample collection, and E. Fichot and C. Suffridge for providing seawater samples for method optimization. We thank B. Hassanzadeh, R. Iturriaga, and D. Monteverde for comments and relevant discussions. **Funding:** This project was founded by the Marie Curie Actions–International Outgoing Fellowships (project 253970), the U.S. National Science Foundation grant OCE1335269, the Simons Foundation award 509727, and the Gordon and Betty Moore Foundation Marine Microbiology Initiative award 3779. J.A. and J.M.G. were supported by the Spanish project HOTMIX (CTM2011-30010-C02-MAR). The University of Dundee is a registered Scottish charity, no. SC015096. **Author contributions:** L.G.-C. and S.A.S.-W. designed the study. L.G.-C., S.A.S.-W., and J.M.G. planned the sampling locations and ancillary parameters to be measured during the cruise. S.A.S.-W., L.G.-C., L.S.C., and B.S. contributed to the development of the retinal oxime analytical technique, and D.W. to the Bchl-*a* measurements. L.G.-C., J.A.R., N.M.L., and D.W. analyzed and did calculations for the solar energy capture data. J.A. was the scientific chief during the Mediterranean–East Atlantic Ocean cruise and provided the Chl-*a* and flow cytometry data. L.G.-C., J.A.R., N.M.L., L.S.C., D.W., B.S., J.A., J.A.F., J.M.G., and S.A.S.-W. analyzed the data and contributed to the writing of the paper. **Competing interests:** J.A.R. is a director of and shareholder in Scottish Bioenergy Cooperative Ventures Limited. The authors declare that they have no other competing interests. **Data and materials availability:** All data needed to evaluate the conclusions in the paper are present in the paper and/or the Supplementary Materials. Additional data related to this paper may be requested from the authors.

Submitted 4 February 2019
Accepted 28 June 2019
Published 7 August 2019
10.1126/sciadv.aaw8855

**Citation:** L. Gómez-Consarnau, J. A. Raven, N. M. Levine, L. S. Cutter, D. Wang, B. Seegers, J. Arístegui, J. A. Fuhrman, J. M. Gasol, S. A. Sañudo-Wilhelmy, Microbial rhodopsins are major contributors to the solar energy captured in the sea. *Sci. Adv.* **5**, eaaw8855 (2019).